# A mathematical model of the Calvin photosynthesis cycle

Pettersson, Gösta; Ryde-Pettersson, Ulf

*Published in:*
European Journal of Biochemistry

*DOI:*
10.1111/j.1432-1033.1988.tb14242.x

1988

*Document Version:*
Publisher's PDF, also known as Version of record

Eur. J. Biochem. 175, 661 – 672 (1988)


# A mathematical model of the Calvin photosynthesis cycle

Gösta PETTERSSON and Ulf RYDE-PETTERSSON

Avdelningen för Biokemi, Kemicentrum, Lunds Universitet, Lund

(Received March 28, 1988) – EJB 88 0348

1. A mathematical model is presented for photosynthetic carbohydrate formation in $C_3$ plants under conditions of light and carbon dioxide saturation. The model considers reactions of the Calvin cycle with triose phosphate export and starch production as main output processes, and treats concentrations of NADPH, $NAD^+$, $CO_2$, and $H^+$ as fixed parameters of the system. Using equilibrium approximations for all reaction steps close to equilibrium, steady-state and transient-state relationships are derived which may be used for calculation of reaction fluxes and concentrations of the 13 carbohydrate cycle intermediates, glucose 6-phosphate, glucose 1-phosphate, ATP, ADP, and inorganic (ortho)phosphate.

2. Predictions of the model were examined with the assumption that photosynthate export from the chloroplast occurs to a medium containing orthophosphate as the only exchangeable metabolite. The results indicate that the Calvin cycle may operate in a single dynamically stable steady state when the external concentration of orthophosphate does not exceed 1.9 mM. At higher concentrations of the external metabolite, the reaction system exhibits overload breakdown; the excessive rate of photosynthate export deprives the system of cycle intermediates such that the cycle activity progressively approaches zero.

3. Reactant concentrations calculated for the stable steady state that may obtain are in satisfactory agreement with those observed experimentally, and the model accounts with surprising accuracy for experimentally observed effects of external orthophosphate on the steady-state cycle activity and rate of starch production.

4. Control analyses are reported which show that most of the non-equilibrium enzymes in the system have a strong regulatory influence on the steady-state level of all of the cycle intermediates. Substrate concentration control coefficients for cycle enzymes may be positive, such that an increase in activity of an enzyme may raise the steady-state concentration of the substrate is consumes.

5. Under optimal external conditions (0.15 – 0.5 mM orthophosphate), reaction flux in the Calvin cycle is controlled mainly by ATP synthetase and sedoheptulose bisphosphatase; the cycle activity approaches the maximum velocity that can be supported by the latter enzyme. At lower concentrations of external orthophosphate the cycle activity is controlled almost exclusively by the phosphate translocator. At high external orthophosphate concentrations the phosphate translocator resumes predominant control, but also other non-equilibrium enzymes gain strong flux control with one notable exception: ribulosebisphosphate carboxylase has no significant regulatory influence on the cycle activity under conditions of light and $CO_2$ saturation, nor does it control the concentration of any cycle intermediate other than its substrate.

The regulation of the reductive pentose phosphate pathway (the Calvin cycle) for photosynthetic carbohydrate formation in $C_3$ plants has been the subject of extensive experimental studies [1 – 4]. Theoretical investigations of the dynamic behaviour of this central metabolic pathway have been more sparse, due probably to its complexity; the Calvin cycle involves enzymes acting on 13 cycle intermediates in a complex network of reactions (Scheme 1) and is dependent on input processes supplying ATP, NADPH, and $CO_2$ to the reaction system, as well as on output processes withdrawing cycle intermediates from the system. Mathematical models of photosynthesis in $C_3$ plants have been presented which incorporate simplified features of the Calvin cycle [5 – 9], but no attempt has been made to elucidate the dynamic and regulatory properties of the cycle by application of modern control theory [10, 11].

Since the Calvin cycle leads to net synthesis of cycle intermediates, analyses of its kinetic behaviour should include consideration of the output processes which withdraw cycle intermediates from the system. We have recently shown by such considerations that the steady-state cycle activity might be controlled with exceptional versatility and strength through the kinetic interplay of the reaction steps that account for the partitioning of reaction flux between output and recycling of a cycle intermediate [12]. With the simplifying assumption that triose phosphate export from the stromal solution represents the only significant output process, a model was derived which provided some insight into the dynamic principles by which external control variables (such as the cytosolic concentration of orthophosphate) may affect the steady-state

*Correspondence to* G. Pettersson, Avdelningen för Biokemi, Kemicentrum, Box 124, S-221 00 Lund, Sweden

*Abbreviations.* The following non-standard abbreviations are used in equations, figures and tables: PGA, 3-phosphoglyceric acid; BPGA, 2,3-bisphosphoglyceric acid; GAP, glyceraldehyde 3-phosphate; DHAP, dihydroxyacetone phosphate; FBP, fructose 1,6-bisphosphate; F6P, fructose 6-phosphate; G6P, glucose 6-phosphate; G1P, glucose 1-phosphate; E4P, erythrose 4-phosphate; SBP, sedoheptulose 1,7-bisphosphate; S7P, sedoheptulose 7-phosphate; R5P, ribose 5-phosphate; X5P, xylulose 5-phosphate; Ru5P, ribulose 5-phosphate; RuBP, ribulose 1,5-bisphosphate.

*Enzymes.* Fructose bisphosphatase (EC 3.1.3.11); sedoheptulose bisphosphatase (EC 3.1.3.37); ribulose-5-phosphate kinase (EC 2.7.1.19); ribulosebisphosphate carboxylase (EC 4.1.1.39); ADP-glucose pyrophosphorylase (EC 2.7.7.27).

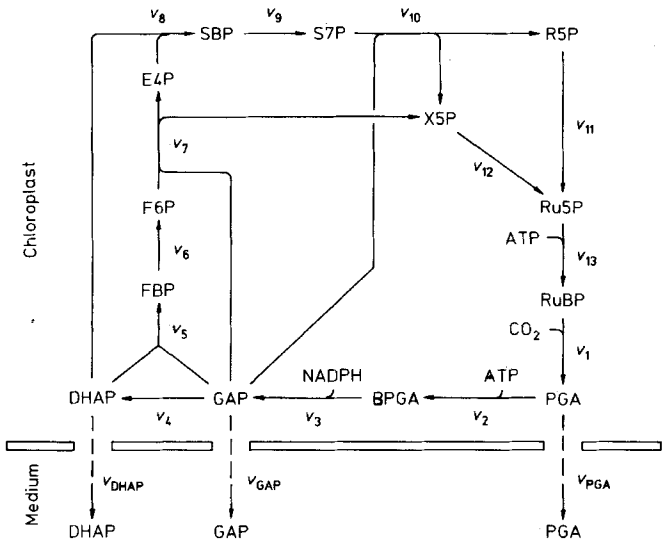


Scheme 1. *The Calvin photosynthesis cycle and steps of photosynthate export*

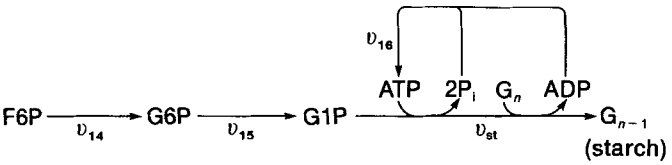


Scheme 2. *Starch production from fructose 6-phosphate and regeneration of ATP*

cycle activity [13]. The model was much too simple, however, to provide any reliable information on the effects of internal control variables such as the stromal concentrations of orthophosphate, ATP, cycle intermediates, and cycle enzymes.

We now wish to put forward a more elaborate model for the Calvin cycle which considers the regulation of the system by such internal control variables, and which incorporates starch production as an additional output process. This model would seem to be sufficiently detailed to form the basis for realistic tests of the kinetic behaviour and control properties of the reaction system. In the present investigation, such analyses are reported primarily for the dependence of the steady-state cycle activity on the concentration of external orthophosphate under conditions of light and carbon dioxide saturation.

## THEORY

### *Reaction system considered*

Scheme 1 depicts the 13 enzymically catalysed reaction steps constituting the Calvin cycle for photosynthetic carbohydrate formation in $C_3$ plants. The reactions involving $CO_2$, ATP, and NADPH are input steps which supply the cycle with reactants for net synthesis of triose phosphates according to the stoichiometric relationship

$$3\,CO_2 + 6\,NADPH + 9\,ATP \rightarrow \text{Triose phosphate} + 6\,NADP^+ + 9\,ADP + P_i \quad (1)$$

where $P_i$ denotes inorganic phosphate (orthophosphate). ATP is assumed to be produced through the action of ATP synthetase on ADP and orthophosphate, as indicated in Scheme 2. The transport processes leading to export of 3-phosphoglycerate, glyceraldehyde 3-phosphate, and dihydroxyacetone phosphate from the chloroplast to the cytosol are included as output steps in Scheme 1. Starch production from fructose 6-phosphate by the sequence of reactions shown in Scheme 2 will be considered as an additional output process, proceeding within the chloroplast.

Table 1. *Fixed stoichiometric parameters of the model*

| Metabolite | Concentration | Reference |
|---|---|---|
| | mM | |
| NADPH | 0.21 | [14] |
| $NAD^+$ | 0.29 | [14] |
| $CO_2$ | >0.2 | – |
| $c_P$ | 15 | [15] |
| $c_A$ | 0.5 | [15] |
| pH (medium) | 7.6 | [16] |
| pH (stroma) | 7.9 | [16] |

### *Concentration variables considered*

The reaction system defined by Schemes 1 and 2 involves 22 non-enzymic reactants. Since the model now presented is intended to illustrate the internal and output control of the Calvin cycle under conditions of saturating light and carbon dioxide, concentrations of four of these reactants (NADPH, $NADP^+$, $CO_2$, and $H^+$) will be regarded as fixed parameters determined by external processes and exhibiting the values indicated in Table 1. Two of the concentration variables ([ATP] and [ADP]), further, are interrelated through the conservation equation

$$c_A = [ATP] + [ADP] \quad (2)$$

where $c_A$ denotes the total concentration of the two adenylate nucleotides. It therefore suffices to consider one of these variables (say [ATP]) as a state variable of the system.

The export of Calvin cycle intermediates from the chloroplast is mediated by the phosphate translocator of the chloroplast membrane and is associated with a counter-import of orthophosphate such that the total stromal concentration of phosphate remains constant [17]. This means that an additional fixed parameter ($c_P$) is defined by the phosphate conservation equation

$$\begin{aligned} c_P = [P_i] &+ [PGA] + 2[BPGA] + [GAP] + [DHAP] \\ &+ 2[FBP] + [F6P] + [E4P] + 2[SBP] \\ &+ [S7P] + [X5P] + [R5P] + [Ru5P] \\ &+ 2[RuBP] + [G6P] + [G1P] + [ATP]. \end{aligned} \quad (3)$$

We have chosen values of 15 mM and 0.5 mM, respectively, for the parameters $c_P$ and $c_A$ [16].

Eqn (3) can be used to calculate the stromal concentration ($[P_i]$) of orthophosphate, provided that magnitudes of the remaining 16 concentration variables in this equation are known. Denoting velocities of the cycle reactions and output steps as in Schemes 1 and 2, the time dependence of the latter variables can be expressed as

$$\frac{d[PGA]}{dt} = 2v_1 - v_2 - v_{PGA} \quad (4)$$

$$\frac{d[BPGA]}{dt} = v_2 - v_3 \quad (5)$$

$$\frac{d[GAP]}{dt} = v_3 - v_4 - v_5 - v_7 - v_{10} - v_{GAP} \quad (6)$$

Table 2. *Equilibrium constants for reaction steps in Schemes 1 and 2* Estimates referring to 25° C of equilibrium constants defined by Eqns (20–30)

| Constant | Value | Unit | Reference |
|---|---|---|---|
| $q_2$ | $3.1\times10^{-4}$ | | [18] |
| $q_3$ | $1.6\times10^{7}$ | | [18] |
| $q_4$ | 22 | | [18] |
| $q_5$ | 7.1 | $mM^{-1}$ | [18] |
| $q_7$ | 0.084 | | [18] |
| $q_8$ | 13 | $mM^{-1}$ | [18] |
| $q_{10}$ | 0.85 | | [18] |
| $q_{11}$ | 0.40 | | [18] |
| $q_{12}$ | 0.67 | | [18] |
| $q_{14}$ | 2.3 | | [18] |
| $q_{15}$ | 0.058 | | [21] |

$$\frac{d[DHAP]}{dt} = v_4 - v_5 - v_8 - v_{DHAP} \quad (7)$$

$$\frac{d[FBP]}{dt} = v_5 - v_6 \quad (8)$$

$$\frac{d[F6P]}{dt} = v_6 - v_7 - v_{14} \quad (9)$$

$$\frac{d[E4P]}{dt} = v_7 - v_8 \quad (10)$$

$$\frac{d[SBP]}{dt} = v_8 - v_9 \quad (11)$$

$$\frac{d[S7P]}{dt} = v_9 - v_{10} \quad (12)$$

$$\frac{d[X5P]}{dt} = v_7 + v_{10} - v_{12} \quad (13)$$

$$\frac{d[R5P]}{dt} = v_{10} - v_{11} \quad (14)$$

$$\frac{d[Ru5P]}{dt} = v_{11} + v_{12} - v_{13} \quad (15)$$

*Equilibrium approximation applied*

Calculations of mass action ratios have indicated that four of the Calvin cycle reactions (those with rates $v_1$, $v_6$, $v_9$, and $v_{13}$ in Scheme 1) are much displaced from equilibrium in illuminated chloroplasts, whereas other reaction steps are relatively close to equilibrium [18–20]. Since only non-equilibrium steps are of primary regulatory interest [2], reaction steps close to equilibrium will be assumed to be at equilibrium such that

$$[BPGA][ADP] = q_2\,[PGA][ATP] \quad (20)$$

$$[GAP][NADP^+][P_i] = q_3\,[BPGA][NADPH][H^+] \quad (21)$$

$$[DHAP] = q_4\,[GAP] \quad (22)$$

$$[FBP] = q_5\,[GAP][DHAP] \quad (23)$$

$$[X5P][E4P] = q_7\,[GAP][F6P] \quad (24)$$

$$[SBP] = q_8\,[DHAP][E4P] \quad (25)$$

$$[X5P][R5P] = q_{10}\,[GAP][S7P] \quad (26)$$

$$[Ru5P] = q_{11}\,[R5P] \quad (27)$$

$$[Ru5P] = q_{12}\,[X5P]. \quad (28)$$

Equilibrium approximations can be analogously applied to the first two reaction steps in Scheme 2, such that

$$[G6P] = q_{14}[F6P] \quad (29)$$

$$[G1P] = q_{15}[G6P]. \quad (30)$$

Equilibrium constant values used in this work are listed in Table 2.

*Rate equations for non-equilibrium cycle steps*

Non-equilibrium steps in the Calvin cycle are assumed to conform to the rate equations

$$v_1 = \frac{V_1[RuBP]}{[RuBP] + K_{m1}\cdot\left(1 + \frac{[PGA]}{K_{i11}} + \frac{[FBP]}{K_{i12}} + \frac{[SBP]}{K_{i13}} + \frac{[P_i]}{K_{i14}} + \frac{[NADPH]}{K_{i15}}\right)} \quad (31)$$

$$v_6 = \frac{V_6[FBP]}{[FBP] + K_{m6}\cdot\left(1 + \frac{[F6P]}{K_{i61}} + \frac{[P_i]}{K_{i62}}\right)} \quad (32)$$

$$v_9 = \frac{V_9[SBP]}{[SBP] + K_{m9}\cdot\left(1 + \frac{[P_i]}{K_{i9}}\right)} \quad (33)$$

$$v_{13} = \frac{V_{13}[Ru5P][ATP]}{\left[[Ru5P] + K_{m131}\cdot\left(1 + \frac{[PGA]}{K_{i131}} + \frac{[RuBP]}{K_{i132}} + \frac{[P_i]}{K_{i133}}\right)\right]\cdot\left[[ATP]\cdot\left(1 + \frac{[ADP]}{K_{i134}}\right) + K_{m132}\cdot\left(1 + \frac{[ADP]}{K_{i135}}\right)\right]} \quad (34)$$

$$\frac{d[RuBP]}{dt} = v_{13} - v_1 \quad (16)$$

$$\frac{d[G6P]}{dt} = v_{14} - v_{15} \quad (17)$$

$$\frac{d[G1P]}{dt} = v_{15} - v_{st} \quad (18)$$

$$\frac{d[ATP]}{dt} = v_{16} - v_2 - v_{13} - v_{st}. \quad (19)$$

with the parameter values indicated in Table 3.

Eqn (31) applies for saturating concentrations of carbon dioxide and accounts for reported inhibitory effects of 3-phosphoglycerate, fructose bisphosphate, sedoheptulose bisphosphate, orthophosphate, and NADPH on the catalytic activity of the fully activated form of ribulosebisphosphate carboxylase [29]. Eqns (32–34), similarly, are based on available literature data for the action of, respectively, fructose

bisphosphatase, sedoheptulose bisphosphatase, and ribulose-5-phosphate kinase in their fully activated form.

Fructose bisphosphatase has been reported to exhibit deviations from Michaelis-Menten kinetics in the presence of inhibitory concentrations of fructose 6-phosphate [33]. Eqn (32) does not account for such a non-Michaelis-Menten rate behaviour of the enzyme but, for the $K_{i61}$ value now chosen, provides a satisfactory approximate description of the inhibitory effect of fructose 6-phosphate at concentrations up to 2 mM.

*Rate equations for input and output processes*

ATP synthesis through the action of ATP synthetase is assumed [26, 27] to adhere to the rate equation

$$v_{16} = \frac{V_{16}[\mathrm{ADP}][\mathrm{P_i}]}{([\mathrm{ADP}] + K_{m161})([\mathrm{P_i}] + K_{m162})}. \quad (35)$$

The action of the phosphate translocator is assumed to conform to the kinetic model proposed by Giersch [35]. If photosynthate export occurs to a reaction medium containing orthophosphate as the only transferable metabolite, rates of the three export steps considered in Scheme 1 may be expressed as

$$v_{\mathrm{PGA}} = \frac{V_{ex}[\mathrm{PGA}]}{N \cdot K_{\mathrm{PGA}}} \quad (36)$$

$$v_{\mathrm{GAP}} = \frac{V_{ex}[\mathrm{GAP}]}{N \cdot K_{\mathrm{GAP}}} \quad (37)$$

$$v_{\mathrm{DHAP}} = \frac{V_{ex}[\mathrm{DHAP}]}{N \cdot K_{\mathrm{DHAP}}} \quad (38)$$

where

$$N = 1 + \left(1 + \frac{K_{P_{ext}}}{[P_{ext}]}\right) \cdot \left(\frac{[P_i]}{K_{P_i}} + \frac{[\mathrm{PGA}]}{K_{\mathrm{PGA}}} + \frac{[\mathrm{GAP}]}{K_{\mathrm{GAP}}} + \frac{[\mathrm{DHAP}]}{K_{\mathrm{DHAP}}}\right). \quad (39)$$

$P_{ext}$ denotes external orthophosphate, and $K_{\mathrm{ligand}}$ represents the apparent dissociation constant for the complex formed between the phosphate translocator and the respective ligand. For convenience, we will introduce the quantity $v_{ex}$ defined by

$$v_{ex} = v_{\mathrm{PGA}} + v_{\mathrm{GAP}} + v_{\mathrm{DHAP}} \quad (40)$$

to denote the net rate of photosynthate export. According to this kinetic model for the phosphate translocator, $v_{ex}$ will equal the rate of orthophosphate import from the external medium to the chloroplast.

Starch production in chloroplasts is rate-limited by the action of ADP-glucose pyrophosphorylase on glucose 1-phosphate and ATP [36]. The enzymic reaction is inhibited by ADP and orthophosphate, and activated by 3-phosphoglycerate, fructose 6-phosphate, and fructose bisphosphate [37]. The corresponding rate equation has not been experimentally characterized in full detail, but is assumed to be given by

$$v_{st} = \frac{V_{st}[\mathrm{G1P}][\mathrm{ATP}]}{\left[[\mathrm{G1P}] + K_{mst1}\right] \cdot \left[\left(1 + \frac{[\mathrm{ADP}]}{K_{ist}}\right) \cdot \left([\mathrm{ATP}] + K_{mst2}\right) + \frac{K_{mst2}[\mathrm{P_i}]}{K_{ast1}[\mathrm{PGA}] + K_{ast2}[\mathrm{F6P}] + K_{ast3}[\mathrm{FBP}]}\right]}. \quad (41)$$

Eqn (41) accounts for the experimentally observed antagonistic effects of orthophosphate and activators. Estimates of the activation parameters ($K_{asti}$) have been chosen such that Eqn (41) provides a reasonably good fit to kinetic data reported for physiological concentrations of the activators [37].

Table 3. *Kinetic parameter values used in the model*

| Parameter | Value | Reference |
|---|---|---|
| | μmol · h$^{-1}$ · (mg Chl)$^{-1}$ | |
| $V_1$ | 340 | [22] |
| $V_6$ | 200 | [23] |
| $V_9$ | 40 | [24] |
| $V_{13}$ | 1000 | [25] |
| $V_{16}$ | 350 | [26, 27] |
| $V_{st}$ | 40 | [28] |
| $V_{ex}$ | 250 | [15] |
| | mM | |
| $K_{m1}$ | 0.02 | [29] |
| $K_{m6}$ | 0.03 | [30] |
| $K_{m9}$ | 0.013 | [31] |
| $K_{m131}$ | 0.05 | [25] |
| $K_{m132}$ | 0.05 | [25] |
| $K_{m161}$ | 0.014 | [26] |
| $K_{m162}$ | 0.30 | [27] |
| $K_{mst1}$ | 0.08 | (see text) |
| $K_{mst2}$ | 0.08 | (see text) |
| $K_{\mathrm{PGA}}$ | 0.25 | [17, 32] |
| $K_{\mathrm{GAP}}$ | 0.075 | [17, 32] |
| $K_{\mathrm{DHAP}}$ | 0.077 | [17, 32] |
| $K_{P_i}$ | 0.63 | [17, 32] |
| $K_{P_{ext}}$ | 0.74 | [17, 32] |
| $K_{i11}$ | 0.84 | [29] |
| $K_{i12}$ | 0.04 | [29] |
| $K_{i13}$ | 0.075 | [29] |
| $K_{i14}$ | 0.90 | [29] |
| $K_{i15}$ | 0.07 | [29] |
| $K_{i61}$ | 0.7 | [33] |
| $K_{i62}$ | 12 | [30] |
| $K_{i9}$ | 12 | [34] |
| $K_{i131}$ | 2 | [25] |
| $K_{i132}$ | 0.7 | [25] |
| $K_{i133}$ | 4 | [25] |
| $K_{i1344}$ | 2.5 | [25] |
| $K_{i135}$ | 0.4 | [25] |
| $K_{ist}$ | 10 | (see text) |
| $K_{ast1}$ | 0.1 | (see text) |
| $K_{ast2}$ | 0.02 | (see text) |
| $K_{ast3}$ | 0.02 | (see text) |

Estimates used for parameters in Eqns (35–40) are included in Table 3. All parameter values in Table 3 have been chosen (or calculated) such that they should be representative for the operation of chloroplasts at a stromal pH of 7.9, assumed to correspond to a pH of 7.6 in the external reaction medium [16]. Consistent with common practise in experimental work, rate parameters and reaction velocities are expressed in relative units (μmol substrate consumed h$^{-1}$ mg chlorophyll$^{-1}$). When required (e.g. to fix the time scale for reactions in the transient state), they were converted into absolute units using an estimate of 30 μl/mg chlorophyll for the volume of the stromal solution [16].

*Steady-state solution*

Under steady-state conditions, time derivatives of all concentration variables become zero. It then follows from Eqns (4–19) that

$$v_1 = v \tag{42}$$

$$v_6 = \frac{v}{3} + v_{st} \tag{43}$$

$$v_9 = \frac{v}{3} \tag{44}$$

$$v_{13} = v \tag{45}$$

$$v_{16} = 3v + v_{st} - v_{PGA} \tag{46}$$

$$v = 3v_{ex} + 6v_{st} \tag{47}$$

where $v$ denotes the cycle activity as measured by the rate of $CO_2$ fixation. Eqns (2), (3) and (20–47) constitute a set of simultaneous equations which can be solved to give the steady-state values of $v$ and of the 18 concentration variables considered in the present model. The non-linearity of these simultaneous equations implies that more than one solution may obtain and that no practically applicable analytical solution can be derived. Results described below were obtained by numerical solution of the equations using standard methods [38] for computer-programmed root determinations.

*Transient-state solution*

Since equilibrium approximations are applied, the transient-state kinetics of the reaction system will be determined exclusively by the rates $v_i$ of the non-equilibrium steps. Eliminating all $v_i$ referring to equilibrium steps, Eqns (4–19) can be reduced to

$$\frac{dy_i}{dt} = F_i;\ i = 1,\ldots,5 \tag{48}$$

where

$$y_1 = [\text{RuBP}] \tag{49}$$

$$y_2 = [\text{F6P}] + [\text{G6P}] + [\text{G1P}] + [\text{E4P}] + [\text{SBP}] \tag{50}$$

$$y_3 = [\text{R5P}] + [\text{Ru5P}] + [\text{X5P}] + [\text{F6P}] + [\text{G6P}] + [\text{G1P}] + 2[\text{S7P}] \tag{51}$$

$$y_4 = [\text{PGA}] + [\text{BPGA}] + [\text{GAP}] + [\text{DHAP}] + 2[\text{FBP}] + [\text{SBP}] - [\text{F6P}] - [\text{G6P}] - [\text{G1P}] - [\text{S7P}] \tag{52}$$

$$y_5 = [\text{ATP}] - [\text{PGA}] \tag{53}$$

$$F_1 = v_{13} - v_1 \tag{54}$$

$$F_2 = v_6 - v_9 - v_{st} \tag{55}$$

$$F_3 = v_6 + 2v_9 - v_{13} - v_{st} \tag{56}$$

$$F_4 = 2v_1 + v_{st} - v_{ex} - 2v_9 - 3v_6 \tag{57}$$

$$F_5 = v_{16} + v_{PGA} - 2v_1 - v_{13} - v_{st}. \tag{58}$$

Eqns (2), (3) and (48–58) implicitely define the time-dependence of all concentration variables considered in the model. This time-dependence can be formally attributed to [RuBP] ($s_1$) and four additional variables $s_j$, i.e. $s_2$ = [DHAP], $s_3$ = [F6P], $s_4$ = [Ru5P], and $s_5$ = [ATP]. Using Eqns (20–30) for elimination of other variables, Eqn (48) may be written as

$$A_{ji} \cdot \frac{ds_j}{dt} = F_i;\ i,j = 1,\ldots,5 \tag{59}$$

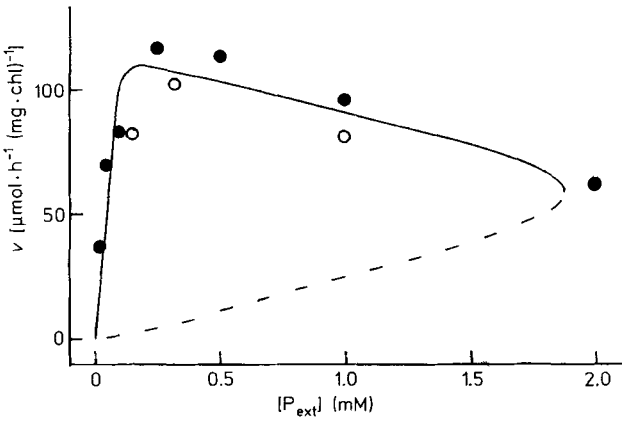


Fig. 1. *Effect of external orthophosphate on the Calvin cycle activity.* Cycle velocities ($v$) predicted by the model for the two steady states (full and dashed curves) that may obtain at external orthophosphate ($P_{ext}$) concentrations below 1.9 mM. Experimental rate data obtained with illuminated isolated chloroplasts by Flügge et al. [41] (●) and Heldt et al. [40] (○) are included for comparison

where $A_{ji}$ represent rationale functions of $s_j$ and parameters of the system as detailed in the Appendix.

Eqn (59) can be readily solved by elementary algebra to provide explicite (although rather complex) expressions for $ds_j/dt$, $j = 1,\ldots,5$. The transient-state rate behaviour of the system may then be determined for arbitrary initial conditions by numerical integration [38] of these expressions and Eqns (2) and (3).

## RESULTS

*Steady states of the reaction system*

According to Eqns (36–39), the activity of the phosphate translocator (and hence the steady-state Calvin cycle activity $v$) is dependent on the concentration ($[P_{ext}]$) of orthophosphate outside the chloroplast. Fig. 1 shows the variation of $v$ with $[P_{ext}]$ as predicted by the steady-state kinetic model described in the theoretical section. There is a critical singularity value of $[P_{ext}]$ (about 1.9 mM) for which the reaction system in Schemes 1 and 2 exhibits a uniquely defined steady state corresponding to a cycle activity of about 60 rate units (μmol $CO_2$ fixed $h^{-1}$ mg chlorophyll$^{-1}$). For lower values of $[P_{ext}]$, the system may exist in two distinct steady states. One yields a cycle activity increasing monotonously within the range 0–60 rate units with increasing $[P_{ext}]$; this will be referred to as the low-velocity case (dashed curve in Fig. 1). The second steady state is characterized by higher cycle activities (high-velocity case); $v$ passes through a maximum of about 110 rate units, which is obtained at an external orthophosphate concentration of about 0.2 mM. For $[P_{ext}] > 1.9$ mM, the reaction system in Schemes 1 and 2 cannot operate in a steady state according to the present model.

Since no analytical solution can be provided for description of the rate behaviour of the reaction system, the stability of the two steady states was analysed numerically for a series of representative values of the parameter $[P_{ext}]$. Such analyses were performed by examination of the eigenvalues of the Jacobian for the system [39], as well as by perturbation tests based on the transient-state kinetic model described in the theoretical section. Both methods consistently indicated that the low-velocity steady state is dynamically unstable, whereas

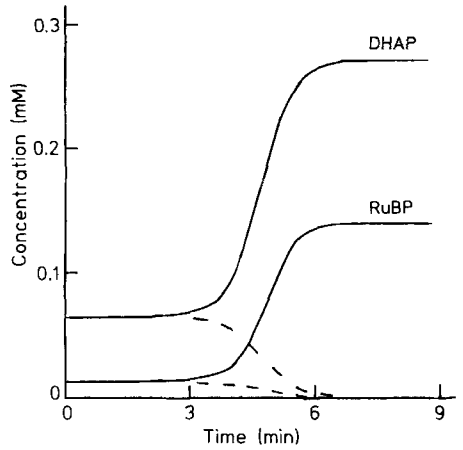


Fig. 2. *Stability test for the low-velocity steady state.* Trajectories calculated for the reaction system in Schemes 1 and 2 when all concentration variables were initially set to their low-velocity steady-state values except for [RuBP] which was set to 101% (full curves) or 99% (dashed curves) of its low-velocity steady-state value

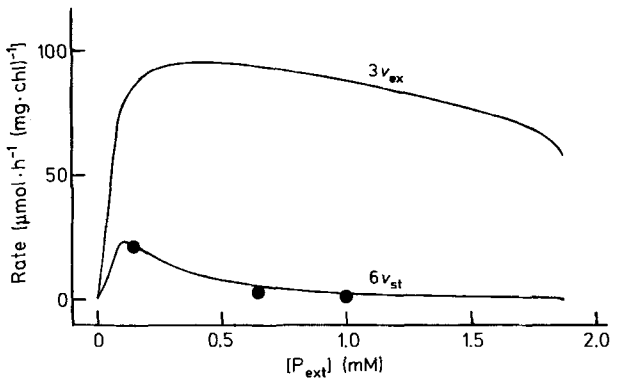


Fig. 3. *Effect of external orthophosphate on the output of photosynthate from the Calvin cycle.* Steady-state reaction fluxes in $C_1$ equivalents for photosynthate export ($3v_{ex}$) from the chloroplast and starch production ($6v_{st}$) within the chloroplast. Reported [40] experimental data for starch production in illuminated isolated chloroplasts (●) are included for comparison

the high-velocity steady state was found to be asymptotically (but not globally) stable. Results of a typical perturbation test are shown in Fig. 2. They illustrate that minor perturbations of the reaction system in its low-velocity steady state cause the system to move towards either the high-velocity steady state or a trivial stationary state in which the concentrations of all cycle intermediates are zero, the transitions being completed within a few minutes.

The observation that the low-velocity steady state is dynamically unstable corroborates the tentative conclusions drawn from our previous analyses of the kinetic structure of the Calvin cycle [12, 13] and implies that this state cannot be of significant biological interest. Further characterization of the predictions of the present model, therefore, was restricted to the high-velocity steady-state case.

### *Comparison with experimental rate data*

The stable steady-state rate behaviour predicted by the model is compared in Fig. 1 with reported [40, 41] experimental data for the effect of external orthophosphate on the Calvin

Table 4. *Metabolite levels in the Calvin cycle*
Metabolite concentrations predicted by the model for an external orthophosphate concentration of 0.5 mM compared with those observed experimentally in illuminated chloroplasts under such conditions

| Metabolite | Calculated concentration | Observed concentration | |
|---|---|---|---|
| | | [19] | [43] |
| | mM | | |
| PGA | 0.59 | 2.15 | 6.0 |
| BPGA | 0.001 | – | – |
| GAP | 0.01 | 0.17 | 0.33 |
| DHAP | 0.27 | | |
| FBP | 0.024 | 0.11 | 0.29 |
| F6P | 1.36 | 0.36 | 3.7 |
| G6P | 3.12 | 0.46 | |
| G1P | 0.18 | | |
| SBP | 0.13 | 0.20 | 0.15 |
| S7P | 0.22 | 0.56 | – |
| E4P | 0.04 | – | – |
| X5P | 0.04 | 0.08 | – |
| R5P | 0.06 | | |
| Ru5P | 0.02 | | |
| RuBP | 0.14 | 0.45 | 0.57 |
| ATP | 0.39 | 0.12 | – |
| $P_{in}$ | 8.1 | 3.2 | 7.0 |

cycle activity in illuminated isolated chloroplasts. Inspection of the data shows that the model accounts with surprising accuracy for the observations made. Not only is the stimulation of the cycle activity by increasing low (less than 0.2 mM) orthophosphate concentrations adequately reproduced, but the model also provides an excellent description of the inhibition caused by higher concentrations of the external metabolite.

As indicated by Eqn (47), the steady-state flux of $C_1$ equivalents generated by $CO_2$ fixation in the Calvin cycle is assumed by Schemes 1 and 2 to be partitioned between photosynthate export ($3v_{ex}$) and starch production ($6v_{st}$). Fig. 3 shows the predictions of the model with regard to the effect of external orthophosphate on the steady-state flux in the respective output process. The results are in most satisfactory agreement with the empirical rate data reported by Flügge et al. for starch production in illuminated chloroplasts [41] and are consistent also with the evidence indicating that starch production at low concentrations of external orthophosphate may account for up to 30% of the total amount of $CO_2$ fixed [42].

### *Steady-state concentrations of metabolites*

The model was applied to calculate the magnitude of all concentration variables in the stable steady state that obtains at an external orthophosphate concentration of 0.5 mM. The results in Table 4 show that metabolite levels thus calculated are in reasonable agreement with those observed experimentally in illuminating chloroplasts operating in reaction media containing 0.5 mM orthophosphate. Fig. 4A–D illustrates the predictions of the model with regard to the effect of external orthophosphate on the steady-state values of the concentration variables. The level of one cycle intermediate

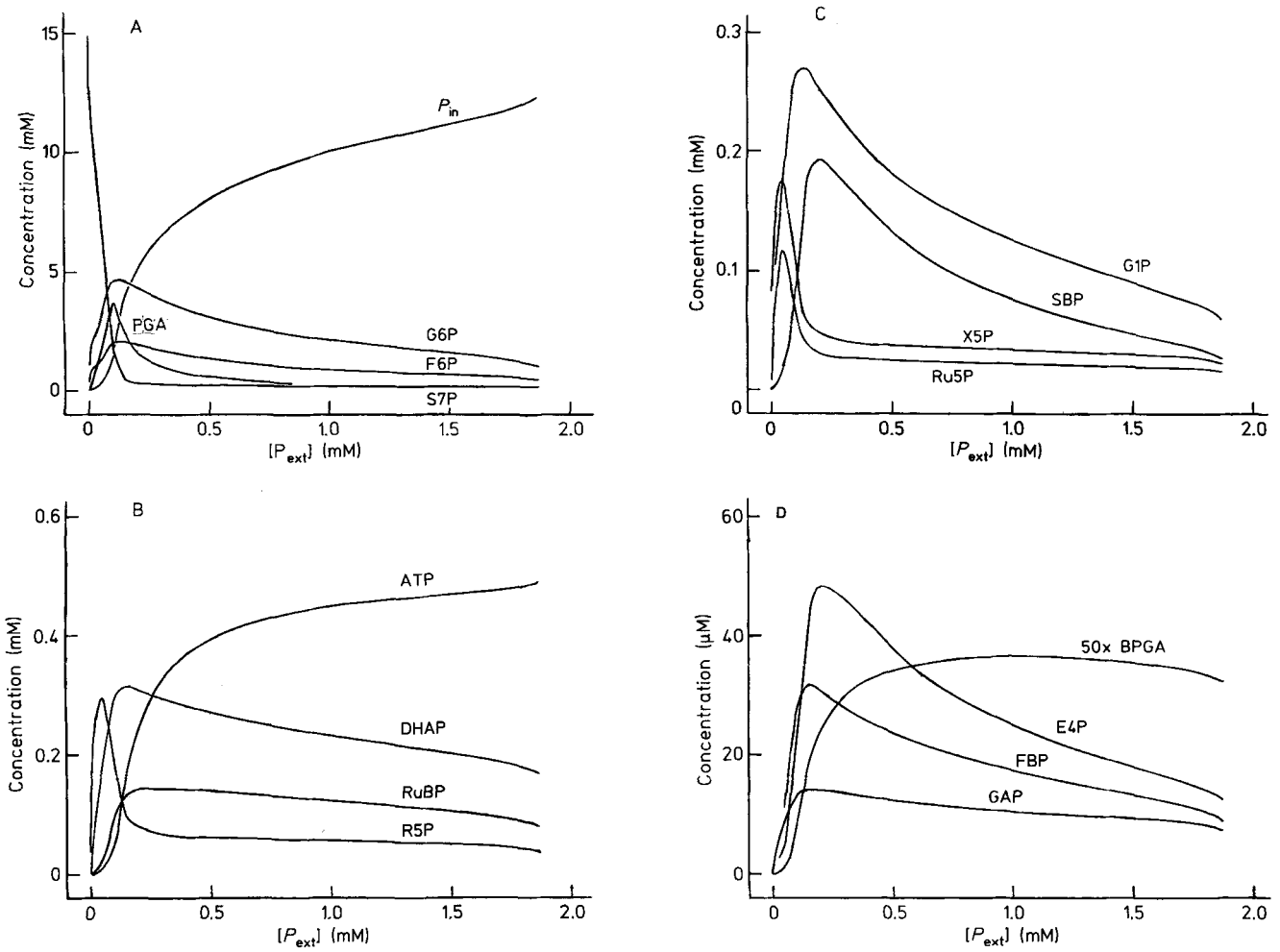


Fig. 4. *Effect of external orthophosphate on the steady-state levels of metabolites.* Metabolite concentrations predicted by the model for the reaction system in Schemes 1 and 2

(sedoheptulose 7-phosphate) decreases monotonously with increasing concentrations of external orthophosphate, and the levels of ATP and internal orthophosphate steadily increase. The amplification factor for the latter metabolite is typically of the order of 10, such that a 0.1 mM change of the external orthophosphate concentration causes an about 1 mM change of the stromal concentration of the metabolite.

Levels of other metabolites exhibit more complex profiles and pass through maxima which in most cases are reached at external orthophosphate concentrations within the range 0.05 – 0.2 mM.

*Control data for the reaction system*

Dimensionless control coefficients $\mathbf{C}_p^x$ describing the change of a system variable $x$ (reaction flux or metabolite concentration) caused by variation of a system parameter $p$ (constants in Tables 1 – 3 or the external concentration of orthophosphate) can be defined [44] as

$$\mathbf{C}_p^x = \frac{\delta x}{\delta p} \cdot \frac{p}{x} = \frac{\delta \ln x}{\delta \ln p}. \qquad (60)$$

Such control data were determined by numerical differentiation [38] of the stable steady-state solution obtaining for the reaction system in Schemes 1 and 2 according to the present model; some typical results are reported in Tables 5 and 6.

Table 5 shows the control matrix describing how maximum activities of non-equilibrium enzymes in the system (the phosphate translocator is considered as an enzyme catalysing a transport step) affect the steady-state metabolite concentrations that obtain at an external orthophosphate concentration of 0.5 mM. Table 6 shows corresponding control data for the steady-state cycle activity at different concentrations of external orthophosphate. The implications of data in Tables 5 and 6 will be considered in the Discussion.

## DISCUSSION

*Basic mathematical approach*

Description of the Calvin cycle from the point of view of reaction kinetics is a formidable task. Even if concentrations of enzymes, NADPH, $NAD^+$, $CO_2$, and $H^+$ are considered as fixed parameters, the reaction system defined by Schemes 1 and 2 will involve 7 independent concentration variables. The time-dependence of these variables is governed by a set of differential equations (Eqns 4 – 19) containing complex non-linear expressions such as those in Eqns (31 – 41). The dynamic behaviour and control properties of a system of that complexity cannot be reliably established by intuitive

Table 5. *Enzyme control of metabolite concentrations*
Control coefficients defined by Eqn (60) calculated for the steady state of the reaction system in Schemes 1 and 2 at an external orthophosphate concentration of 0.5 mM

| Variable ($x$) | Parameter ($p$) | | | | | | |
|---|---|---|---|---|---|---|---|
| | $V_1$ | $V_6$ | $V_9$ | $V_{13}$ | $V_{16}$ | $V_{ex}$ | $V_{st}$ |
| [PGA] | 0.09 | −0.30 | 3.90 | 0.66 | −2.34 | −1.87 | −0.13 |
| [BPGA] | 0.05 | −0.79 | 0.63 | 0.13 | −0.40 | 0.33 | 0.06 |
| [GAP] } [DHAP] | 0.01 | −0.42 | −0.15 | −0.02 | 0.91 | −0.32 | −0.02 |
| [FBP] | 0.02 | −0.84 | −0.31 | −0.03 | 1.82 | −0.63 | −0.04 |
| [F6P] } [G6P] } [G1P] | 0.01 | 0.73 | −1.79 | −0.27 | 2.22 | −0.79 | −0.12 |
| [SBP] | 0.07 | 0.07 | −3.70 | 0.56 | 4.34 | −1.19 | −0.14 |
| [S7P] | −0.09 | 0.07 | 3.37 | −1.71 | −1.51 | −0.14 | 0.00 |
| [E4P] | 0.06 | 0.48 | −3.55 | 0.58 | 3.43 | −0.88 | −0.12 |
| [X5P] } [R5P] } [Ru5P] | −0.04 | −0.17 | 1.61 | −0.86 | −0.30 | −0.23 | −0.01 |
| [RuBP] | −1.39 | −0.20 | 0.81 | 0.27 | 0.69 | −0.17 | −0.01 |
| [ATP] | −0.01 | −0.10 | −0.70 | −0.11 | 0.41 | 0.47 | 0.04 |
| [$P_{in}$] | 0.04 | −0.37 | 0.78 | 0.14 | −1.31 | 0.64 | 0.08 |

Table 6. *Enzyme control of the Calvin cycle activity*
Control coefficients defined by Eqn (60) calculated for the steady-state cycle flux ($v$) in the reaction system in Schemes 1 and 2 at different concentrations of external orthophosphate, [$P_{ext}$]

| Parameter ($p$) | Value at [$P_{ext}$] (mM) = | | | | | |
|---|---|---|---|---|---|---|
| | 0.05 | 0.15 | 0.5 | 1.0 | 1.5 | 1.8 |
| $V_1$ | 0.00 | 0.00 | 0.01 | 0.02 | 0.03 | 0.1 |
| $V_6$ | −0.01 | −0.02 | 0.03 | 0.15 | 0.50 | 3.9 |
| $V_9$ | −0.15 | 0.29 | 0.43 | 0.60 | 0.94 | 3.8 |
| $V_{13}$ | −0.07 | 0.03 | 0.07 | 0.17 | 0.38 | 2.1 |
| $V_{16}$ | 0.02 | 0.65 | 0.69 | 0.73 | 0.91 | 2.9 |
| $V_{ex}$ | 0.98 | 0.05 | −0.20 | −0.64 | −1.72 | −11.6 |
| $V_{st}$ | 0.23 | 0.00 | −0.02 | −0.03 | −0.05 | −0.2 |

reasoning, but requires characterization by strict analysis based on mathematical modelling.

In the model now presented, equilibrium approximations are used for all reaction steps close to equilibrium, an approach which previously has been successfully applied in control studies of the glycolytic pathway [45]. We have refrained, however, from using the standard approach of introducing linearizing first-order assumptions to reduce the complexity of the rate equations for enzymatically catalysed reaction steps (Eqns 31 – 41), a main reason being that such assumptions are insufficient to eliminate all sources of non-linearity in the system. Furthermore, physiological concentrations of substrates for non-equilibrium enzymes in the Calvin cycle can hardly be considered as negligible in comparison to the corresponding $K_m$ values (see Tables 3 and 4). Finally, our previous model studies [13] have indicated that the dynamic and control properties of the Calvin cycle may be fundamentally dependent on the saturation behaviour of critical enzymic reaction steps. Hence it would seem obvious that the consequences of this saturation behaviour should be characterized rather than neglected.

The consequent persisting non-linearity of the differential equations forming the basis for the present model precludes the derivation (even under steady-state conditions) of explicite analytical expressions for the concentration variables and reaction fluxes. Application of the model, therefore, requires computer-programmed numerical methods for solution of the differential equations and for the determination of various control measures. This practical and theroretical inconvenience is a prize one has to pay in order to obtain reliable information on the dynamic behaviour and control properties of the complex system considered.

### *Modes of operation of the Calvin cycle*

Hahn [8] recently concluded from a mathematical model of leaf carbon metabolism that the Calvin cycle may operate in an infinite number of steady states. That conclusion may hold true in the trivial sense that the steady-state activity of the cycle is dependent on a multitude of parameters which, in principle, may attain an infinite number of values. For any given set of values of these parameters, however, there must be a finite number of steady-state modes of operation of the system. This follows from the fact that the dynamic state of the system is defined by a finite number of kinetic differential equations.

Fixed parameter values used in this investigation (Tables 1 – 3) are realistic and supported by experimental evidence; they have been selected from presently available literature data to be representative for the operation of illuminated chloroplasts at saturating $CO_2$ concentrations in reaction media containing orthophosphate as the only external metabolite that may be transferred to the stromal solution through the action of the phosphate translocator. For these parameter values, the present model prescribes that steady-state conditions may or may not obtain depending on the concentration of external orthophosphate (which represents a varied parameter of the model). When the latter concentration is below a certain singularity value (about 1.9 mM), steady-state requirements can be met at two distinct levels of Calvin cycle intermediates. The level leading to the lower cycle activity, however, corresponds to a dynamically unstable steady state of insignificant biological interest. It seems reasonable to con-

clude, therefore, that the Calvin cycle is unlikely to operate in more than a single stable steady state under physiological conditions.

When the external orthophosphate concentration exceeds the critical singularity value, steady-state conditions cannot obtain; the system will be in a transient state where the excessive rate of photosynthate export deprives the chloroplast of Calvin cycle intermediates such that the cycle activity progressively approaches zero. Evidence for such a non-steady-state mode of operation of the Calvin cycle has been obtained by Flügge et al. [41] with isolated chloroplasts in reaction media containing 2 mM orthophosphate. A certain rate of $CO_2$-dependent $O_2$ evolution was observed (cf. Fig. 1), but only trace amounts of crucial cycle intermediates could be detected after illumination of the chloroplasts for 4 min.

The effect of external orthophosphate on the Calvin cycle activity (Fig. 1) has been generally described in terms of rate stimulation over the concentration range 0 – 0.2 mM and rate inhibition at higher orthophosphate concentrations. The present results indicate that it could be of importance in certain contexts to make a clear distinction between the inhibition characterizing the steady-state operation of the reaction system at external orthophosphate concentrations within the range 0.2 – 1.9 mM (Fig. 1) and the inhibition reflecting the 'overload breakdown' [46] of the system at external orthophosphate concentrations above the singularity value.

*Reliability of the model*

There are four main sources of uncertainty as to the accuracy of the predictions of the model now presented. Firstly, the equilibrium assumptions applied are approximations which do introduce errors with regard to the detailed levels of metabolites in the reaction system. Secondly, rate equations applied for the enzymic non-equilibrium steps in some instances (e.g. Eqns 35 and 41) may turn out to be oversimplified when more detailed kinetic information on the corresponding enzymes ultimately becomes available. Thirdly, the model considers only the system in Schemes 1 and 2 and disregards other stromal reactions and processes (e.g. ADP dismutation and starch degradation) which may affect the levels of metabolites in the system. Finally, model data now reported are based on a multitude of parameter estimates (Tables 1 – 3) which in some cases may be subjected to considerable experimental error. The present results, therefore, should be interpreted with some caution, at least as concerns the predicted detailed metabolite levels.

On the other hand, it is apparent from Figs 1 and 3 that the model accounts excellently for the Calvin cycle activities and rates of starch production observed experimentally in illuminated chloroplasts under different conditions. This provides a pragmatic justification for the simplifying approximations introduced and indicates that the model can be reliably used for analysis of the main dynamic and regulatory properties of the reaction system considered. Such analyses could be directed towards any problem relating to the internal control structure and parameter dependence of the system, but this investigation has focused on the regulatory effects of external orthophosphate and the enzyme maximum activities.

*Control of reaction fluxes by external orthophosphate*

The Calvin cycle activity can be affected by metabolic events outside the chloroplast, being dependent, for instance, on the external concentration of orthophosphate [41, 47 – 50]. This dependence has been proposed to reflect effects of the external metabolite on the transport capacity of the phosphate translocator [51]. Results in Figs 1 and 3 lend strong support to that idea by establishing that cycle activities and rates of starch production calculated on the basis of this proposal (i.e. using Eqns 36 – 39) exhibit the experimentally observed variation with the external orthophosphate concentration.

Discussion of the regulatory role played by the phosphate translocator have usually been founded on the assumptions that an increase in concentration of external orthophosphate leads to an increased steady-state rate of photosynthate export and decreased levels of the Calvin cycle intermediates [48, 52 – 55]. Such generalized assumptions may seem intuitively reasonable, but reveal a lack of recognition of the kinetic complexity of the reaction system in Schemes 1 and 2. Eqns (36 – 39) show that the rate of photosynthate export not only exhibits a direct dependence on the external concentration of orthophosphate, but also an indirect dependence deriving from the influence of the external metabolite on the internal concentrations of orthophosphate and the exported cycle intermediates. The net effect of external orthophosphate on the export rate, therefore, cannot be reliably established except by detailed analysis of the reaction system as a whole. Application of the present model indicates (Fig. 3) that the export rate actually may increase or decrease with increasing concentrations of external orthophosphate depending on what concentration range is considered.

Similar considerations apply for the effect of external orthophosphate on metabolite levels in the system (Fig. 4). Concentrations of all cycle intermediates but one may increase or decrease with increasing concentrations of the external metabolite, passing through maxima which occur at different external orthophosphate concentrations with different cycle intermediates and which do not coincide with the maximum exhibited by the rate of photosynthate export. The most obvious correlation between the export rate and metabolite levels in general is the one existing at external orthophosphate concentrations below 0.05 mM. That correlation, however, is in a direction opposite to the one generally assumed, i.e. an increased export rate is associated with increased levels of the cycle intermediates.

It may be concluded from these results that there is no simple way of rationalizing the experimentally observed effects of external orthophosphate on the Calvin cycle activity or the rates of photosynthate export and starch production. Mechanistic explanations for the data in Figs 1 and 3 have to be based on detailed analyses of the flux control exerted by different concentration variables. Such analyses may be performed by application of the model now described, but are beyond the scope of the present investigation.

*Enzyme control of metabolite concentrations*

Results in Table 4 and Fig. 4 show that steady-state metabolite concentrations predicted by the model are in reasonable agreement with those observed experimentally. Concentration control coefficients for the different metabolites may be calculated with regard to any parameter in the system, but are presented (Table 5) only for the enzyme maximum activities in the experimentally typical case that the external orthophosphate concentration equals 0.5 mM. A control matrix such as the one in Table 5 provides basic information on the internal regulatory properties of the system by indicating how metabolite concentrations are affected by variation of factors

than can be directly related to the activity of an individual enzyme (e.g. turnover number, enzyme concentration, or concentrations of modifiers of the enzymic reaction rate).

According to data in Table 5, ADP-glucose pyrophosphorylase (see column for the parameter $V_{st}$) does not strongly control any metabolites in the reaction system. This reflects the fact that starch production represents a rather insignificant output process at the chosen concentration of external orthophosphate (Fig. 3). Ribulosebisphosphate carboxylase ($V_{13}$) is unique among the cycle enzymes in controlling no metabolite strongly except for its substrate (RuBP). The remaining five non-equilibrium enzymes in the system have a relatively pronounced regulatory influence on most or all of the metabolites, which means that the concentration of each metabolite is strongly controlled by several enzymes. This complex control pattern reflects the complex dynamic structure of the Calvin cycle and illustrates the difficulty of interpreting intuitively experimentally observed changes in the metabolite levels. Accumulation of fructose bisphosphate, for example, might certainly be a consequence of an impaired activity of fructose bisphosphate ($\mathbf{C}_{V_6}^{[FBP]} = -0.84$), but could also derive from a decreased activity of the phosphate translocator ($\mathbf{C}_{V_{ex}}^{[FBP]} = -0.63$) or from an increased activity of ATP synthetase ($\mathbf{C}_{V_{16}}^{[FBP]} = 1.82$).

It should be emphasized that the control matrix in Table 5 is quantitatively representative only for the behaviour of the system at external orthophosphate concentrations around 0.5 mM. If the concentration of the external metabolite is raised to 1.7 mM, for example, one gets $\mathbf{C}_{V_6}^{[FBP]} = 0.54$. The latter datum is of interest because it illustrates that fructose bisphosphatase may exhibit a positive concentration control coefficient with regard to its substrate. This means that enhancement of the activity of the enzyme accounting for the consumption of fructose bisphosphate will raise the steady-state concentration of the substrate. Such an apparently paradoxical kinetic situation may arise because the Calvin cycle intermediates are not only substrates for the enzymes they interact with, but also ultimate products of the cycle process thus initiated. Enhancement of the enzymic activity will tend to increase the product concentration and, depending on the properties of the system as a whole, that tendency may or may not be stronger than the tendency to decrease the substrate concentration.

When the external orthophosphate concentration is raised to 1.8 mM, all non-equilibrium cycle enzymes except ribulosebisphosphate carboxylase exhibit positive substrate concentration control coefficients.

*Enzyme control of reaction fluxes*

Despite an extensive debate, uncertainty has remained as to what Calvin cycle enzyme accounts for the main regulation of the cycle activity. Results in Table 6 provide a partly unexpected answer to that question by indicating that (under conditions of light and $CO_2$ saturation) the steady-state cycle activity at low concentrations of external orthophosphate ($P_{ext}$) is not significantly controlled by anyone of the cycle enzymes, but regulated mainly by the phosphate translocator and to some extent also by ADP-glucose pyrophosphorylase. The explanation for this output control of the cycle activity is that the phosphate translocator cannot support photosynthate export at a rate exceeding $V_{ex}[P_{ext}]/K_{P_{ext}}$ (see Eqns 36–39). When $[P_{ext}] \ll K_{P_{ext}}$, the corresponding maximum export flux becomes significantly lower than the reaction fluxes that can be supported by the cycle enzymes. Under such conditions, the phosphate translocator (which accounts for the main output process) will provide a main contribution to the rate-limitation of the steady-state operation of the Calvin cycle; this follows from the fact that the cycle activity must match the rates of the output processes under steady-state conditions.

When the external orthophosphate concentration is raised from 0.05 mM to 0.15 mM, the output control of the system is gradually lost (Table 6). The cycle activity becomes regulated mainly by ATP synthetase, and to a significant extent also by sedoheptulose bisphosphatase. This regulatory situation is maintained for external orthophosphate concentrations up to about 1 mM, where the phosphate translocator resumes predominant control. At even higher concentrations of the external metabolite, significant flux control is gradually gained also by other non-equilibrium enzymes; as might be expected according to our previous analyses of the dynamic structure of the Calvin cycle [12, 13], control strengths of all non-equilibrium enzymes become of unlimited magnitude when the concentration of external orthophosphate approaches the singularity value above which the system cannot operate in a steady state.

The control exerted by ATP synthetase at external orthophosphate concentrations around the optimal value reflects a rate limitation contributed by the relatively low maximum velocity ($V_{16} = 350$ rate units) assigned to the enzyme; according to Eqn (46), the maximum cycle activity that can be supported by ATP synthetase should fall somewhere between $V_{16}/3$ and $V_{16}/2$, i.e. between 120 and 180 rate units. Since the magnitude of $V_{16}$ is known to be strongly light-dependent [56], the present results leave little doubt that ATP synthetase may account for the main light control of the cycle activity.

Available literature data [56] could support the use of $V_{16}$ values considerably higher than 350 rate units, however, and there is a possibility that the value now chosen does not refer to conditions of strict light saturation. Attention, therefore, should be drawn to the control exerted by sedoheptulose bisphosphatase in the same region of optimal cycle activity (Table 6). The low maximum velocity of the latter enzyme ($V_9 = 40$ rate units) corresponds to a maximum cycle activity of 120 rate units (Eqn 44), which is only marginally higher than that observed experimentally. The low activity of sedoheptulose bisphosphatase appears to put a definite limit to the rate of cyclic $CO_2$ fixation under optimal conditions.

A final inference provided by data in Table 6 is that the flux control strength of ribulosebisphosphate carboxylase is completely negligible compared to that of other non-equilibrium enzymes. This result may seem somewhat unexpected, considering the multitude of reports that have attributed an important regulatory function to ribulosebisphosphate carboxylase [57]. That function would not appear to come into play under the conditions of light and $CO_2$ saturation now examined, but might be manifest at physiological concentrations of $CO_2$. The latter and other regulatory problems relating to the parameter dependence of the model now presented will be considered in future studies.

## APPENDIX

Coefficients $A_{ji}$ in Eqn (59) are given by

$$A_{11} = 1$$

$$A_{j1} = 0; j = 2,\ldots,5 \; A_{12} = A_{13} = 0$$

$$A_{14} = -2t_{11}$$

$$A_{15} = 2t_{13}$$

$$A_{22} = t_1(1 + 2q_8s_2)s_3$$

$$A_{23} = -\frac{2t_2s_4}{s_2}$$

$$A_{24} = 2(t_3s_3 + t_4) + t_5 + \frac{t_2s_4}{s_2} + \frac{t_7t_8}{t_6} - t_{10}t_{11}$$

$$A_{25} = (c_{ad} - s_5)\left(\frac{t_{10}s_2}{t_6 + t_9s_2} - \frac{t_7}{t_6}\right)$$

$$A_{32} = t_1(1 + q_8s_2)s_2 + t_{12}$$

$$A_{33} = t^{12}$$

$$A_{34} = t_3s_2 - t_1(1 + 2q_8s_2)s_2t_{11} - t_{12}(1 + t_{11})$$

$$A_{35} = t_{13}[t_{12} + t_1(1 + 2q_8s_2)s_2]$$

$$A_{42} = -\frac{t_1(1 + q_8s_2)s_2s_3}{s_4}$$

$$A_{43} = 4t_2 + t_{14}$$

$$A_{44} = t_{11}t_{15} - 2t_2 - \frac{t_1q_8s_2^2s_3}{s_4}$$

$$A_{45} = -t_{13}t_{15}$$

$$A_{52} = A_{53} = 0$$

$$A_{54} = \frac{c_{ad}t_7s_2(t_{11} - 1)}{t_6s_5} - t_{11}$$

$$A_{55} = 1 + t_{13} + \frac{c_{ad}t_7s_2(1 - t_{13})}{t_6s_5}$$

where

$$t_1 = \frac{q_7q_{12}}{q_4s_4}$$

$$t_2 = \frac{q_4s_4}{q_{10}q_{11}q_{12}s_2}$$

$$t_3 = \frac{q_7q_8q_{12}s_2}{q_4s_4}$$

$$t_4 = \frac{2q_5s_2}{q_4}$$

$$t_5 = 1 + \frac{1}{q_4}$$

$$t_6 = \frac{q_2q_3q_4s_5[\mathrm{NADPH}][\mathrm{H}^+]}{[\mathrm{NADP}^+]}$$

$$t_7 = t_{16}[c_p\text{-}2s_1 - s_5 - (t_4 + t_5)s_2 - t_{12}s_3 - (t_2 + t_{14})s_4 - t_1(1 + 2q_8s_2)s_2s_3]$$

$$t_8 = c_{ad} + (q_2 - 1)s_5$$

$$t_9 = c_{ad} + (2q_2 - 1)s_5$$

$$t_{10} = 2t_4 + t_5 + t_1(1 + 4q_8s_2)s_3 + \frac{t_7t_9}{t_6} - \frac{t_2s_4}{s_2}$$

$$t_{11} = \frac{t_8t_{16}s_2}{t_6}$$

$$t_{12} = 1 + q_{14} + q_{14}q_{15}$$

$$t_{13} = \frac{t_{16}(c_{ad} - s_5)s_2}{t_6}$$

$$t_{14} = 1 + \frac{1}{q_{11}} + \frac{1}{q_{12}}$$

$$t_{15} = \frac{t_1(1 + 2q_8s_2)s_2s_3}{s_4} - 2t_2 - t_{14}$$

$$t_{16} = \frac{t_6}{t_6 + t_9s_2}.$$

This investigation was supported by grants from the Swedish Natural Science Research Council.

## REFERENCES


1. Bassham, J. A. (1979) in *Encyclopaedia of plant physiology* (Gibbs, M. & Latzko, E., eds) vol. 6, pp. 9–30, Springer Verlag, Berlin.
2. Robinson, S. P. & Walker, D. A. (1980) in *The biochemistry of plants* (Hasch, M. D. & Boardman, N. K., eds) vol. 8, pp. 193–236, Academic Press, London.
3. Herold, A. (1980) *New Phytol. 86*, 131–144.
4. Edwards, G. E. & Walker, D. A. (1983) *$C_3$,$C_4$: Mechanisms and cellular and environmental regulation of photosynthesis*, Blackwell Scientific Press, Oxford.
5. Laisk, A. (1973) *Biophysics 18*, 679–684.
6. Milstein, J. & Bremermann, H. J. (1979) *J. Math. Biol. 7*, 99–116.
7. Kaitala, V., Hari, P., Vapaavuori, E. & Salminen, R. (1982) *Ann. Bot. 50*, 385–396.
8. Hahn, B. D. (1984) *Ann. Bot. 54*, 325–339.
9. Laisk, A. & Walker, D. A. (1986) *Proc. R. Soc. Lond. B227*, 281–302.
10. Kacser, H. & Burns, J. A. (1973) in *Rate control of biological processes* (Davies, D. D., ed.) pp. 65–104, Cambridge University Press, London.
11. Heinrich, R. & Rapoport, T. A. (1974) *Eur. J. Biochem. 42*, 89–95.
12. Pettersson, G. & Ryde-Pettersson, U. (1988) *Life Sci. Adv., D7*, 131–136.
13. Pettersson, G. & Ryde-Pettersson, U. (1987) *Eur. J. Biochem. 169*, 423–429.
14. Giersch, C., Heber, U. & Krause, G. H. (1980) in *Plant membrane transport* (Sparswick, R. M., Lucas, W. J. & Daity, J., eds) pp. 65–83, Elsevier, Amsterdam.
15. Lilley, R. M., Chon, C. J., Mosbach, A. M. & Heldt, H. W. (1977) *Biochim. Biophys. Acta 460*, 259–272.
16. Heldt, H. W., Werdan, K., Milovancek, M. & Geller, G. (1973) *Biochim. Biophys. Acta 314*, 224–241.
17. Fliege, R., Flügge, U.-I., Werdan, K. & Heldt, H. W. (1978) *Biochim. Biophys. Acta 502*, 232–247.
18. Bassham, J. A. & Krause, G. H. (1969) *Biochim. Biophys. Acta 189*, 207–221.
19. Portis, A. R., Chon, C. J., Mosbach, A. & Heldt, H. W. (1977) *Biochim. Biophys. Acta 461*, 313–325.
20. Dietz, K. & Heber, U. (1984) *Biochim. Biophys. Acta 767*, 432–443.
21. Colowick, S. P. & Sutherland, E. W. (1942) *J. Biol. Chem. 144*, 423–435.
22. Badger, M. R. & Andrews, T. J. (1974) *Biochem. Biophys. Res. Commun. 60*, 204–210.
23. Charles, S. A. & Halliwell, B. (1981) in *Photosynthesis* (Akoyunoglou, G., ed.) vol. 4, pp. 347–356, Balaban, Philadelphia.
24. Laing, W. A., Stitt, M. & Heldt, H. W. (1981) *Biochim. Biophys. Acta 637*, 348–359.
25. Gardemann, A., Stitt, M. & Heldt, H. W. (1983) *Biochim. Biophys. Acta 722*, 51–60.
26. Davenport, J. W. & McCarty, R. E. (1986) *Biochim. Biophys. Acta 851*, 136–145.
27. Aflalo, C. & Shavit, N. (1983) *FEBS Lett. 154*, 175–179.
28. Latzko, E., Steup, M. & Schächtele, C. (1981) in *Photosynthesis* (Akoyunoglou, G., ed.) vol. 4, pp. 517–528, Balaban, Philadelphia.
29. Badger, M. & Lorimer, G. H. (1981) *Biochemistry 20*, 2219–2225.
30. Charles, S. A. & Halliwell, B. (1980) *Biochem. J. 185*, 689–693.
31. Woodrow, I. E. & Walker, D. A. (1982) *Arch. Biochem. Biophys. 216*, 416–422.
32. Portis, A. R. (1983) *Plant Physiol. 71*, 936–943.
33. Heldt, H. W., Gardemann, A., Gerhardt, R., Herzog, B., Stitt, M. & Wirtz, W. (1984) in *Advances in photosynthesis research* (Sybesma, C., ed.) vol. 3, pp. 617–624, Nijhoff/Junk, Haag.
34. Woodrow, I. E., Murphy, D. J. & Walker, D. A. (1983) *Eur. J. Biochem. 132*, 121–123.
35. Giersch, C. (1977) *Z. Naturforsch. 32C*, 263–270.

36. Preiss, J. (1982) *Annu. Rev. Plant Physiol. 33*, 431–454.
37. Ghosh, H. P. & Preiss, J. (1966) *J. Biol. Chem. 241*, 4491–4504.
38. Fröberg, C.-E. (1970) *Introduction to numeric analysis*, Addison-Wesley, London.
39. Heinrich, R., Rapoport, S. M. & Rapoport, T. A. (1977) *Prog. Biophys. Mol. Biol. 32*, 1–82.
40. Heldt, H. W., Chon, C. J., Maronde, D., Herold, A., Stankovic, Z. S., Walker, D. A., Kraminer, A., Kirk, M. R. & Heber, U. (1977) *Plant Physiol. 59*, 1146–1155.
41. Flügge, U. I., Freisl, M. & Heldt, H. W. (1980) *Plant Physiol. 65*, 574–577.
42. Steup, S., Peavey, D. G. & Gibbs, M. (1976) *Biochem. Biophys. Res. Commun. 72*, 1554–1561.
43. Heldt, H. W., Chon, C. J. & Lorimer, G. H. (1978) *FEBS Lett. 92*, 234–240.
44. Burns, J. A., Cornish-Bowden, A., Groen, A. K., Heinrich, R., Kacser, H., Porteous, J. W., Rapoport, S. M., Rapoport, T. A., Stucki, J. W., Tager, J. M., Wanders, R. J. A. & Westerhoff, H. V. (1985) *Trends Biochem. Sci. 10*, 16.
45. Rapoport, T. A., Heinrich, R., Jacobasch, G. & Rapoport, S. (1974) *Eur. J. Biochem. 42*, 107–120.
46. Reich, J. G. & Selkov, E. E. (1981) *Energy metabolism of the cell*, Academic Press, London.
47. Lilley, R. M., Schwenn, J. D. & Walker, D. A. (1973) *Biochim. Biophys. Acta 325*, 596–604.
48. Herold, A. (1980) *New Phytol. 86*, 131–144.
49. Preiss, J. (1984) *Trends Biochem. Sci. 9*, 24–27.
50. Walker, D. A. & Sivak, M. N. (1986) *Trends Biochem. Sci. 11*, 176–179.
51. Heldt, H. W. (1976) in *Topics in photosynthesis* (Barber, J., ed.) vol. 1, pp. 215–234, Elsevier, Amsterdam.
52. Shen-Hwa, C.-S., Lewis, D. H. & Walker, D. A. (1975) *New Phytol. 74*, 383–392.
53. Herold, A. & Walker, D. A. (1977) in *Handbook of transport across membranes* (Giebisch, G., Tostesan, D. C. & Ussing, H. H., eds) pp. 411–439, Springer Verlag, Heidelberg.
54. Furbank, R. T. & Lilley, R. M. (1980) *Biochim. Biophys. Acta 592*, 65–75.
55. Rao, I. M., Abadia, J. & Terry, N. (1987) in *Progress in photosynthesis research* (Biggens, J., ed.) vol. 3, pp. 751–754, Nijhoff, Dordrecht.
56. Bickel-Sandkötter, S. & Strotmann, H. (1981) *FEBS Lett. 125*, 188–192.
57. Miziorko, H. M. & Lorimer, G. H. (1983) *Annu. Rev. Biochem. 52*, 507–535.